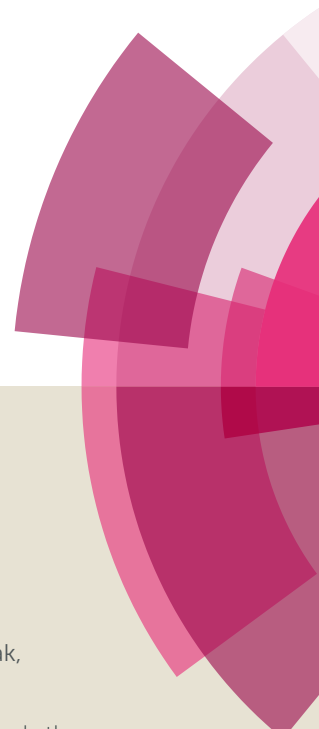


NJC

Accepted Manuscript



This article can be cited before page numbers have been issued, to do this please use: C. Sinha, A. Adak, R. Purkait, S. K. Manna, B. Ghosh and S. Pathak, *New J. Chem.*, 2019, DOI: 10.1039/C8NJ06511J.



This is an Accepted Manuscript, which has been through the Royal Society of Chemistry peer review process and has been accepted for publication.

Accepted Manuscripts are published online shortly after acceptance, before technical editing, formatting and proof reading. Using this free service, authors can make their results available to the community, in citable form, before we publish the edited article. We will replace this Accepted Manuscript with the edited and formatted Advance Article as soon as it is available.

You can find more information about Accepted Manuscripts in the [author guidelines](#).

Please note that technical editing may introduce minor changes to the text and/or graphics, which may alter content. The journal's standard [Terms & Conditions](#) and the ethical guidelines, outlined in our [author and reviewer resource centre](#), still apply. In no event shall the Royal Society of Chemistry be held responsible for any errors or omissions in this Accepted Manuscript or any consequences arising from the use of any information it contains.

Fluorescence sensing and intracellular imaging of Pd²⁺ ion by a novel coumarinyl-rhodamine Schiff base†

Arup Kumar Adak,^{a,b} Rakesh Purkait^b, Saikat Manna,^c Bankim Chandra Ghosh,^d Sudipta Pathak^c and Chittaranjan Sinha^{b*}

^a Department of Chemistry, Bidhannagar College, EB-2, Sector –1, Salt Lake, Kolkata–700064, West Bengal, India.

^b Department of Chemistry, Jadavpur University, Kolkata–700032, West Bengal, India.

^c Department of Chemistry, Haldia Govt. College, Debhog, Haldia, Purba Medinipur–721657, West Bengal, India.

^d Department of Chemistry, Durgapur Govt. College, J. N. Avenue, Durgapur, Paschim Bardhaman –713214, West Bengal, India.

Abstract

Coumarinyl-rhodamine, **HCR**, serves as extremely selective sensor to Pd²⁺ ion in ethanol/H₂O (8:2, v/v, HEPES buffer, pH 7.2) solution and the limit of detection (LOD) is 18.8 nM (3σ method). The free sensor, **HCR**, is weakly emissive and in presence of Pd²⁺, the colour changes from straw to pink with very strong emission at 598 nm in presence of eighteen other cations. The plausible mechanism includes opening of the spirolactam ring of rhodamine upon interaction with Pd²⁺. This is justified by a structure optimization and transition energy calculation by DFT technique. **HCR** undergoes 1:1 complexation with Pd²⁺ that has been confirmed via Job's plot, mass spectra and Bensei-Hildebrand plot (association constant K_a, 9.1×10⁴ M⁻¹). A separate *in*

in vitro experiment shows that **HCR** can specifically perceive Pd²⁺ in MCF7 (Human breast adenocarcinoma) cell lines.

Keywords: Coumarinyl-rhodamine, Pd²⁺-sensor, spirolactam ring opening, live cell imaging, DFT computation.

Corresponding Author: crsjuchem@gmail.com (C. Sinha)

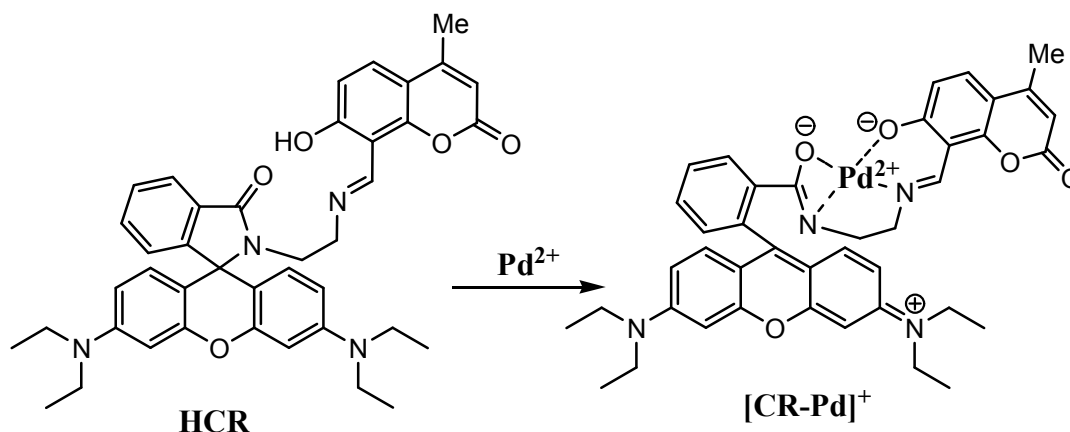
† Electronic supplementary information (ESI) available. See DOI: xxxxxxxxxxxx

1. Introduction

During the past few years, the development of methods for the identification and sensing of platinum group metals (PGMs) has received amazing interest because of their enormous biological, environmental, industrial and chemical significance.¹⁻⁴ Among these, palladium, a precious metal, has become one of the most attractive sensing targets in recent years because of its wide catalytic use in synthesis of organic and pharmaceutical molecules, fuel cells, dental appliances, medical devices, electrical equipments etc.^{5,6} In the Pd-catalysed reactions, it may apprehend that Pd(0) oxidation state may temporarily oxidize or those of Pd(IV) may reduce to the intermediate oxidation state Pd(II) as the reaction proceeds. The final product is often contaminated with impurity of Pd(II) even after rigorous purification. Such contamination in ultratrace level in the industrial products may cause serious health problem. Due to its thiophilic nature, palladium can bind with DNA, proteins and other macromolecules, and disturb a variety of cellular processes.^{7,8} Palladium also hampers the activity of many enzymatic reactions such as alkaline phosphatase, creatine kinase and prolyl hydroxylase (Hypoxia-inducible factor) etc.^{9,10} For these reasons, various analytical techniques are used for the quantitative analysis of

1
2
3 palladium. Popular techniques are inductively coupled plasma-mass spectrometry (ICP-MS),
4 atomic absorption spectrometry (AAS), solid-phase micro-extraction high performance liquid
5 chromatography (SPME-HPLC) and X-ray fluorescence spectroscopy.¹¹⁻¹³ However; these
6 methods require sophisticated highly expensive equipments, extensive sample preparation steps,
7 time-consuming and high salaried experts. Among these different techniques for the analysis of
8 palladium ions, colorimetric and fluorometric techniques are more convenient and dependable
9 for the speedy and sensitive detection of palladium both qualitatively and quantitatively in light
10 of their simplicity, selectivity and sensitivity. Hence, the development of palladium selective
11 fluorescent probes is extremely essential. Pd²⁺, being a heavy transition metal ion with an open
12 shell electronic configuration, is a typical fluorescence quencher.¹⁴ Based upon the ON-OFF¹⁵
13 or OFF-ON^{16,17} mechanism some fluorescent chemosensors and chemodosimeters are
14 synthesized for the identification of palladium species. Towards the design of sensor, the
15 important objectives are the long-wavelength emission and ecofriendly availability of fluorescent
16 chemosensors. With this views Rhodamine functionalized chemosensors are of increasing
17 interest in current years.¹⁸ For the last couple of years we have taken a strategy to design
18 Rhodamine derivatives for the identification of trace level of Pd; allyl ether Schiff base of
19 Rhodamine¹⁹ has been tested for detection of total Pd at 50 nM while allyl ether hydrazone
20 Rhodamine is capable to detect as low as 95 nM concentration²⁰ at pH 7.2. The performance of
21 Rhodamine derivatives has inspired us to synthesize newer chemosensor those could able to
22 detect even lower concentration of Pd(II). For further accomplishment, we have selected two
23 fluorogenic units, coumarin and rhodamine, to combine together in a single molecule, (E)-3',6'-
24 bis(diethylamino)-2-(2-(((7-hydroxy-4-methyl-2-oxo-2H-chromen-8-yl)methylene)amino)ethyl)
25 spiro[isoindoline-1,9'-xanthen]-3-one (**HCR**) (**Scheme 1**) and has been used for the detection of
26
27
28
29
30
31
32
33
34
35
36
37
38
39
40
41
42
43
44
45
46
47
48
49
50
51
52
53
54
55
56
57
58
59
60

Pd²⁺. **HCR** is nearly non-emissive while its complexation with Pd²⁺ makes powerfully fluorescent motif within the red wavelength region (598 nm) that may be due to opening of spirolactam ring of rhodamine. The potential application of the ligand (**HCR**) has been carried out by intracellular imaging in the MCF7 (human breast adenocarcinoma) cell line in presence of exogenous palladium ions.



Scheme 1: Proposed sensing mechanism of Pd²⁺-selective sensor **HCR** ($\lambda_{em} = 598$ nm for the complex).

2. Experimental section

2.1 Materials and methods

Rhodamine B (Sigma-Aldrich) and resorcinol, ethylene diamine, ethyl acetoacetate (Spectrochem) were used as received. All other organic chemicals and inorganic salts were acquired from Merck and utilized without further purification. Purified water was collected from Milli-Q water (Millipore). Following instruments were used for different physicochemical measurements : Perkin-Elmer 2400 Series-II CHN analyzer, Perkin Elmer, USA for elemental analyses; Perkin Elmer Lambda 25 spectrophotometer for absorption spectral measurements;

Perkin Elmer spectrofluorimeter model LS55 for emission spectral studies; Perkin Elmer LX-1 FTIR spectrophotometer used for IR spectral collection; Bruker (AC) 300 MHz FT-NMR spectrometer utilizing TMS as an internal standard for NMR spectra; Water HRMS model XEVO-G2QTOF#YCA351 spectrometer used for mass spectra. Data were collected at room temperature.

The test sample and reference were excited at the identical wavelength. From the area of the fluorescence spectra (using available software in the instrument) the fluorescence quantum yield of the experimental sample was calculated using the equation,

$$\frac{\phi_S}{\phi_R} = \left[\frac{F_S}{F_R} \right] \times \left[\frac{A_R}{A_S} \right] \times \left[\frac{\eta_S^2}{\eta_R^2} \right] \quad \dots(1)$$

Where, ϕ_R and ϕ_S are the fluorescence quantum yield of the reference and samples; F_R and F_S are the respective areas under emission spectra of the reference and sample respectively. A_R and A_S are the absorbance of the reference and sample at the excitation wave length. η_R and η_S are the refractive index of the solvent used for the reference and the sample. Fluorescein (reported quantum yield, $\phi_R = 0.79$ in 0.1M NaOH²¹) was used as reference sample.

2.2 Synthesis of probe, HCR

4-Methyl-7-hydroxy-8-formylcoumarin (**A**)²² and N-(rhodamine-B)lactam-1,2-ethylenediamine (**B**)²³ were synthesized by reported methods. A suspension of **B** (1.0 equiv) in dry EtOH (10 ml) was stirred at 80°C with 4-methyl-7-hydroxy-8-formyl Coumarin (**A**) (1.0 equiv) in the same solvent (10 ml) under inert (N₂) environment for 2 h; and an orange-yellow colored crystalline product was separated. The solvent extraction using ethyl acetate/brine water system was performed followed by chromatographic separation over silica gel using ethyl acetate/petroleum

ether (1:1 v/v) solvent mixture to elute the desired product, **HCR**. Yield: 75%, m.p.: 145-147°C, ¹H NMR (300 MHz, CDCl₃) δ 8.62 (s, 1H), 7.91 (d, *J* = 5 Hz, 1H), 7.44-7.42 (m, 3H), 7.09 (t, *J* = 3 Hz, 1H), 6.70 (d, *J* = 9 Hz, 1H), 6.32-6.45 (m, 6H), 5.98 (s, 1H), 3.51 (t, *J* = 6Hz, 2H), 3.32-3.34 (m, 10H), 2.42 (s, 3H), 1.16 (t, *J* = 6.81 Hz, 12H) (**ESI**[†], **Fig. S1**); ¹³C NMR (75 MHz, CDCl₃) δ 172.4, 168.3, 162.3, 160.6, 160.5, 155.0, 153.6, 153.4, 153.3, 148.9, 132.6, 130.8, 129.5, 128.7, 128.1, 123.8, 123.0, 117.7, 109.2, 108.3, 105.2, 105.0, 97.7, 64.9, 53.5, 44.4, 40.1, 18.9, 12.6. (**ESI**[†], **Fig. S2**); MS ES⁺, *m/z* calculated for C₄₁H₄₂N₄O₅: 670.32; found: 671.16 [M+H]⁺ (**ESI**[†], **Fig. S3**); IR (KBr pellet, cm⁻¹): 3180, 1570 (**ESI**[†], **Fig. S4**).

2.3 UV-vis and fluorescence spectral studies

Ethanol solution (5 ml) of **HCR** (3.35 mg, 0.001 mmol) was used as stock solution; 100 μL of this stock of **HCR** was diluted utilizing 2 ml ethanol/H₂O (8:2, v/v) containing HEPES buffer (pH 7.2). Independently, a Pd²⁺ solution was prepared by warming PdCl₂ (1.77 mg, 0.001 mmol) in minimum volume of DMSO and diluted to 10 ml by adding water. Microlitre quantities of Pd²⁺ solution was slowly poured to the **HCR** solution prepared above for spectral measurement. Excitation wavelength of 545 nm (excitation slit = 5.0 and emission slit = 5.0) was used for fluorescence study.

2.4 Theoretical computation

Optimized molecular geometries of **HCR** and [CR⁻-Pd²⁺]⁺ complex were generated by DFT/B3LYP technique exploiting Gaussian 09 software.²⁴⁻²⁷ For C, H, N, O basis set of 6-311G were used and for heavy atom Pd the LanL2DZ basis set was used.^{28,29} Vibrational frequency calculations were checked with the optimized geometries which could represent the structures of

the species closer to the actual structure. TD-DFT technique in MeOH using conductor-like polarizable continuum model (CPCM)³⁰⁻³² was employed for theoretical evaluation of UV-vis spectra. The fractional contributions of various groups to the molecular orbital were checked by GAUSSSUM program.³³

2.5 Biological studies

2.5.1 Cell culture

The cells of MCF7, human breast adenocarcinoma cell line, (NCCS, Pune, India) were cultured in CO₂ incubator (5%) at 37°C using DMEM containing fetal bovine serum (FBS) (10%), Kanamycin sulfate (110 mg/L), penicillin (50 units/ml) and streptomycin (50 µg/ml). The cell detachment during cell splitting program was checked by Trypsin-EDTA (1X) solution was used for cell detachment during cell splitting.

2.5.2 Cell viability assay of tetramer peptides

Human breast adenocarcinoma cell line, MCF7 cells were taken in DMEM culture media with 10% fetal bovine serum. Using different concentrations of **HCR** ligand in DMEM medium cell viability assay was performed within ninety six well plates. MTT (3-(4,5-dimethylthiazol-2-yl)-2,5-diphenyltetrazolium bromide) is a colorimetric technique where yellow tetrazole compound gets reduced to purple coloured formazan by reductase enzymes present in living cells while the dead cells are unable to interfere. Formazan was further dissolved in DMSO/MeOH (1:1 (v/v)) and absorbance of each well was measured at 550 nm by micro-plate ELISA reader. Percent of viability was measured from absorbance value. Percentage viability has been calculated as

$$\frac{\{A_{550} \text{ (treated cell)} - A_{550} \text{ (background)}\}}{\{A_{550} \text{ (untreated cell)} - A_{550} \text{ (background)}\}} \times 100.$$

2.5.3 Cellular uptake study by microscopic imaging

Approximately, 2000 MCF7 cells were seeded in DMEM medium containing 10% fetal bovine serum on cover glass bottom disc for overnight before the treatment. Then, the media was removed and 5 μM **HCR** in DMEM containing media was added and incubated for 3 h (DMSO concentration maintained 0.4%). After 3 h of incubation, 5 μM of Pd^{2+} was added and incubated for another 30 min followed by the addition of 4% formaldehyde in PBS buffer for 30 min to fix the cell in each cover glass. Formaldehyde solution was then removed and washed with PBS buffer. Cell imaging was performed by a spinning disc confocal microscope with 40X objective (Olympus) equipped with AndoriXon 3897 EMCCD camera in 568 nm wavelength light.

3. Results and discussions

3.1 Synthesis and characterization of HCR

The probe (E)-3',6'-bis(diethylamino)-2-(2-(((7-hydroxy-4-methyl-2-oxo-2H-chromen-8-yl)methylene)amino)ethyl)spiro[isoindoline-1,9'-xanthen]-3-one (**HCR**) is synthesized by the reaction of 4-methyl-7-hydroxy-8-formyl-Coumarin (**A**) and N-(rhodamine-B)lactam-1,2-ethylenediamine (**B**) (ESI^+ , Scheme S1). Disappearance of $\nu(\text{CHO})$ of **A** at 1651 cm^{-1} and $\nu(\text{NH}_2)$ of **B** in the FTIR spectrum of **HCR** and the strong stretch at 1624 cm^{-1} refers to $\nu(\text{C}=\text{N})$ along with lactone $\nu(\text{COO})$, 1729 cm^{-1} and $\nu(\text{OH})$, 3444 cm^{-1} stretching have confirmed the synthesis of the probe. The mass spectral peak at 671.16 matches to $[\text{M}+\text{H}]^+$ (calculated m/z for $\text{C}_{41}\text{H}_{42}\text{N}_4\text{O}_5$ is 670.32) and supports the elemental composition of **HCR**. The ^1H NMR spectrum of (300 MHz, CDCl_3) shows singlet at 2.42 ppm which is assigned to methyl protons at coumarinyl back bone. Signals at δ 3.53-3.32 ppm refer to methylene protons which are attached

1
2
3 to nitrogen centres. The most deshielded protons at δ 8.62 ppm is assigned to imine proton which
4 proves the formation of Schiff base. The triplet signal at δ 1.16 ppm is due to the presence of –
5 CH_3 protons of ethyl group. All other aromatic-Hs are usual and have been compared with
6 literature data.³⁴ ^{13}C NMR spectrum is difficult to assign due to large number of overlapping C
7 centres. Ester carbonyl and amide carbonyl appear at 172.4 and 168.3 ppm respectively. Peaks at
8 18.9, 12.6 ppm are assigned to two types of methyl groups. The carbons which are attached to
9 nitrogen centers appear at 64.9, 53.5, 44.4, 40.1 ppm. The quaternary carbon appears as highest δ
10 value (64.9 ppm) among said four carbons and has been compared with literature report.³⁵

3.2 Absorption spectroscopic studies

11
12
13
14
15
16
17
18
19
20
21
22
23
24
25
26
27
28
29
30
31
32
33
34
35
36
37
38
39
40
41
42
43
44
45
46
47
48
49
50
51
52
53
54
55
56
57
58
59
60

HCR exhibits absorption in ethanol-water (8:2, v/v; HEPES buffer, pH, 7.2)) at 272, 317, 350 and 414 nm. The addition of following metal ions, for example, Na^+ , K^+ , Ca^{2+} , Mg^{2+} , Ba^{2+} , Al^{3+} , Mn^{2+} , $\text{Fe}^{2+/3+}$, Co^{3+} , Ni^{2+} , Cu^{2+} , Zn^{2+} , Cd^{2+} , Hg^{2+} , Ag^+ , Pb^{2+} , Pt^{2+} , ($\approx 10^{-4}$ M) to **HCR** solution does not show any significant change in visible color under indistinguishable conditions, while on adding Pd^{2+} at even lower concentration ($\approx 10^{-6}$ to 10^{-5} M) shows a reasonable improvement of absorbance at 565 nm and a visible change of colour (**Fig. 1**). Addition of Pd^{2+} to EtOH/ H_2O solution (8:2, v/v, HEPES buffer, pH 7.2) of **HCR**, pale yellow colour of free probe changes to pink with a strong absorption band centered at 565 nm (**Fig. 2**). It is unanimously explained the unique selectivity of **HCR** to Pd^{2+} over other competitive metal ions and the experiment demands easy sensitive naked eye probe for Pd^{2+} .

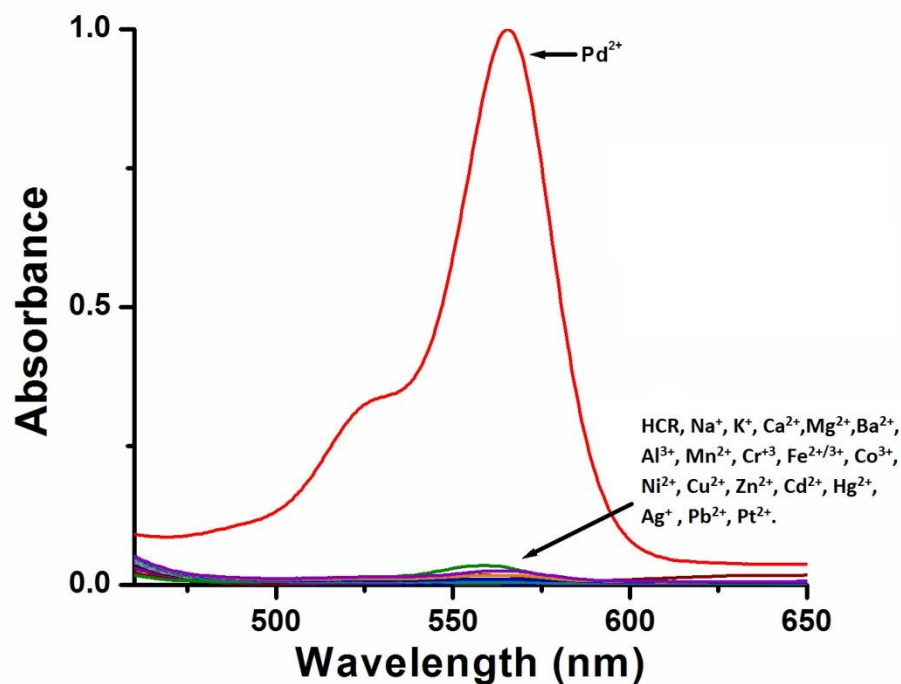


Fig. 1: UV-vis responses of **HCR** to various metal ions in EtOH/H₂O (8:2, v/v, HEPES buffer, pH 7.2). [**HCR**] = 2.0×10^{-5} M, [Pd²⁺] = 1.0×10^{-5} M, [other ions] $\approx 10^{-4}$ M.

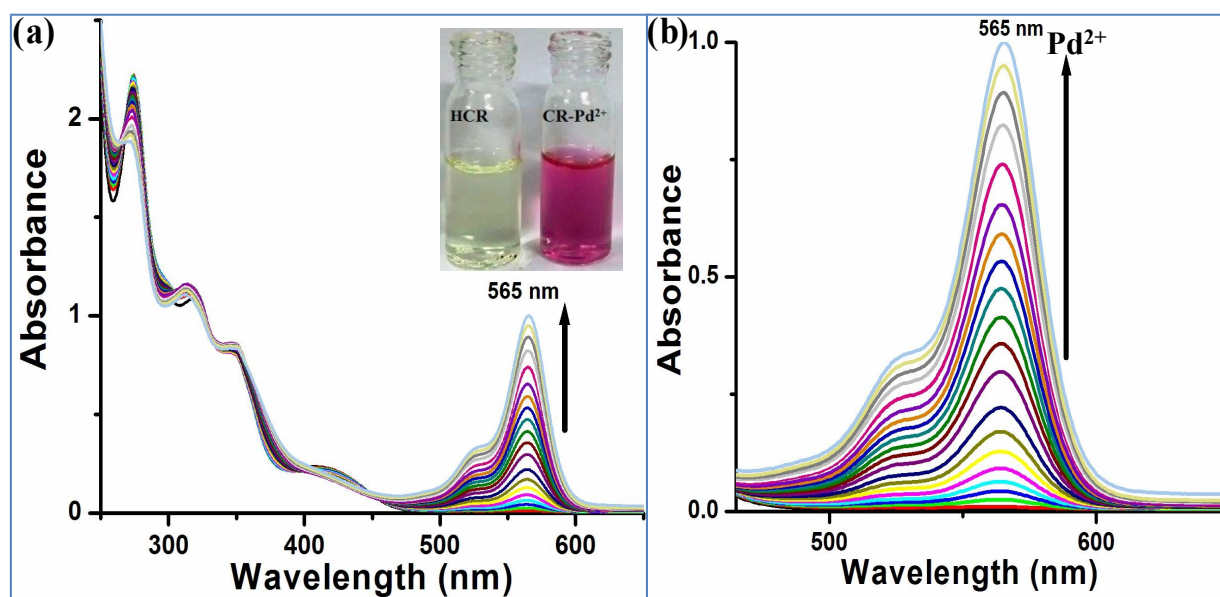


Fig. 2: (a) Variation of UV-vis spectrum of sensor **HCR** (2.0×10^{-5} M) in EtOH/H₂O (8:2 v/v, 20 mM HEPES buffer, pH 7.2) medium on adding of Pd²⁺ ion (0 to 9.5×10^{-6} M with increment of 5.0×10^{-7} M) gradually. (b) Magnification of the relevant portion of (a). Inset: Naked eye view of the sensor solution before and after addition of Pd²⁺ ion.

3.3 Emission spectroscopic studies

The sensor, **HCR**, bears two fluorogenic units, Coumarin and Rhodamine-B; so, our apprehension is that it could be utilized as powerful fluorogenic dyad. With the end goal to additionally explore the selectivity of **HCR** to Pd²⁺, the fluorescence spectral response of **HCR** to the previously mentioned metal ions have been analyzed. Upon addition of Pd²⁺ to the solution of **HCR** a brilliant fluorescence is observed (**Fig. 3**) at 598 nm with high quantum yield of the [CR-Pd²⁺]⁺ complex (Φ , 0.68; fluorescein standard) while **HCR** is very weakly emissive (**Fig. 3**). This demonstrates that **HCR** is extremely selectivity to Pd²⁺ ion. During the titration of **HCR** solution by adding Pd²⁺ ion, the fluorescence intensity at 598 nm gradually increases; excitation at 545 nm enhances the fluorescence intensity by 270 times (**Fig. 4**). The experimental detection limit (LOD) of Pd²⁺ is 18.8 nM (3 σ method, ESI†, **Fig. S5**). Use of a number of the rhodamine functionalized sensor for quantitative identification of Pd²⁺ has been reported; for example, rhodamine bonded azophenol shows LOD 450 nM³⁴, rhodamine-nitro-salicaldehyde Schiff base exhibits LOD 50 nM¹⁹, rhodamine-ethynyl-benzaldehyde gives LOD 191 nM³⁵, rodamine appended oxime is accounted for with LOD 15 nM³⁶, rodamine-benzimidazole gives LOD 21 nM.³⁷ The present probe, **HCR** is astoundingly high sensitive (LOD, 18.8 nM) and it is a potential competitor in Pd²⁺ sensor's club.

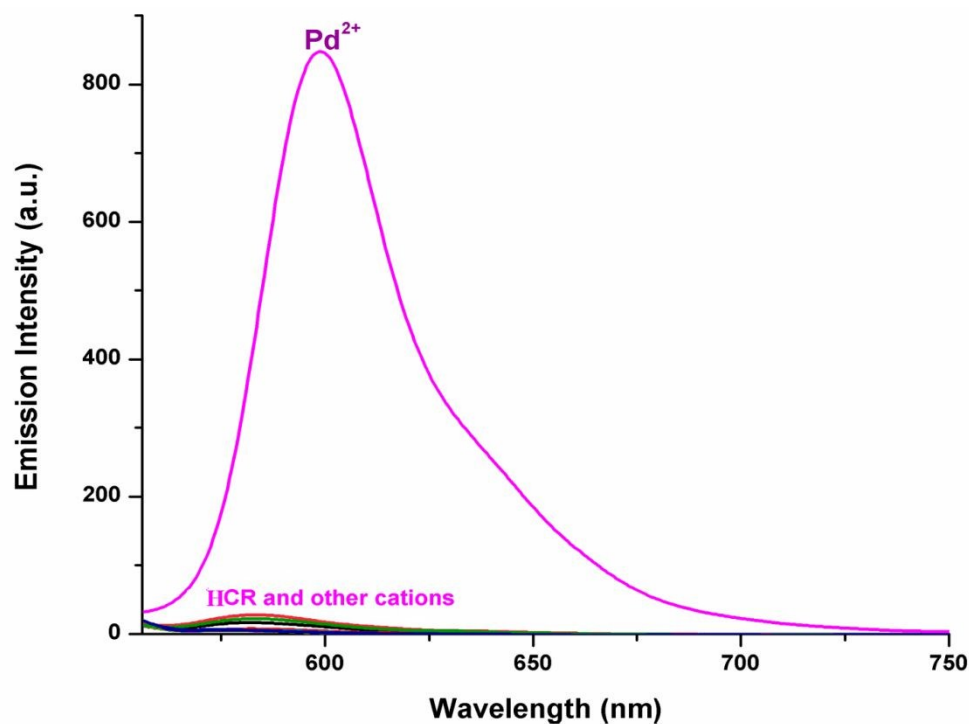


Fig. 3: Emission spectra of **HCR** on adding different metal ions and Pd^{2+} in EtOH/ H_2O (8:2 v/v, 20 mM HEPES buffer, pH 7.2). $[\text{HCR}] = 2.0 \times 10^{-5}$ M, $[\text{Pd}^{2+}] = 1.0 \times 10^{-5}$ M, [other ions] $\approx 10^{-4}$ M.

The complex $[\text{CR}^- - \text{Pd}^{2+}]^+$ shows better excited state stability (τ_{complex} , 1.62 ns) than that of free ligand, HCR only (τ_{HCR} , 0.15 ns) (**Fig. 5**). Enhancement of life time on binding with Pd^{2+} supports the stabilization at excited state by sharing orbitals of metal ion. Hence, Pd^{2+} induced cleavage of the C–O bond with consequent chelation and opening of the spirolactam ring³⁸⁻⁴⁵ (**Scheme 1**).

The pH sensitivity of the emission of HCR shows that there is almost no change in emissivity of the ligand in the pH range 7.0 - 12.0 while in acidic pH 3.0 – 7.0 a substantial intensity change is observed. In presence of Pd^{2+} the ligand does not show any change of emission in the pH range 2.0-12.0 (**Fig. 6**). Hence sensing of Pd^{2+} by **HCR** through fluorescence

enhancement is most suitable in the pH range of 7.0–12.0, which may be attributed solely to a spiro lactam ring opening of the rhodamine moiety caused by Pd^{2+} ion. Thus, Pd^{2+} can be detected in approximately physiological pH ranges in living cells using **HCR**.

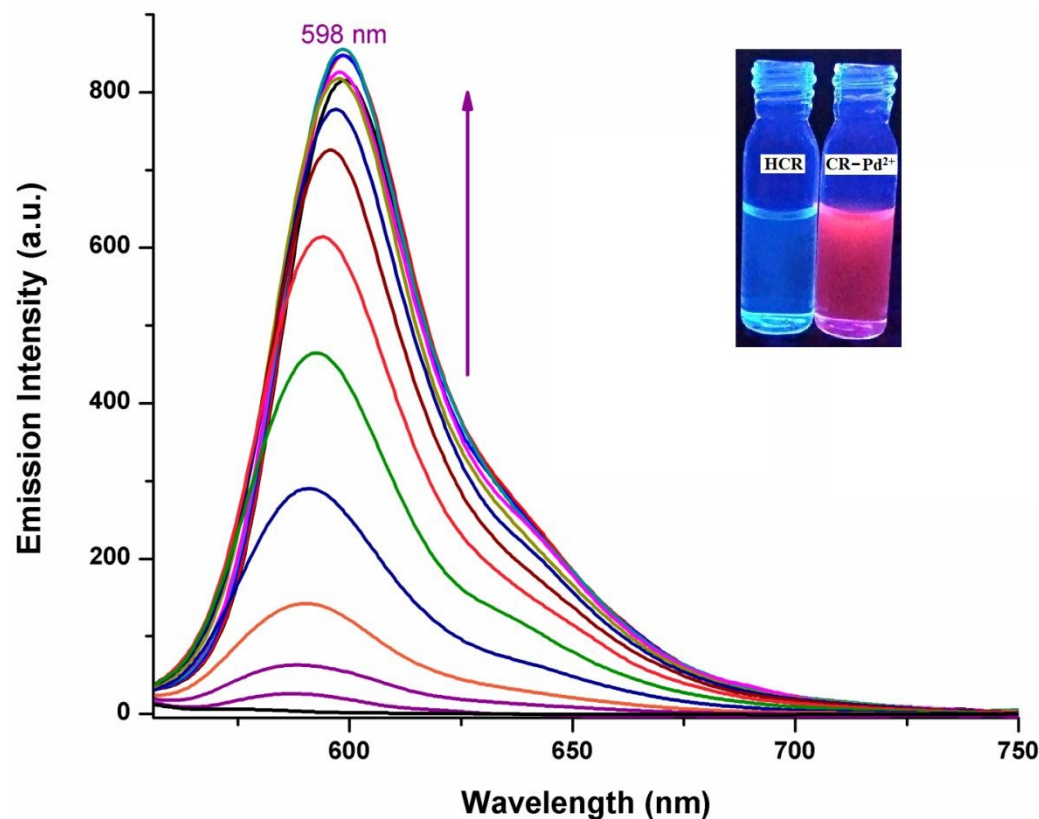


Fig. 4: Alteration in the fluorescence spectra of **HCR** upon the addition of Pd^{2+} at an emission slit of 5 nm; inset: naked eye view of the sensor solution (placed in a UV chamber) in presence and absence of Pd^{2+} ions.

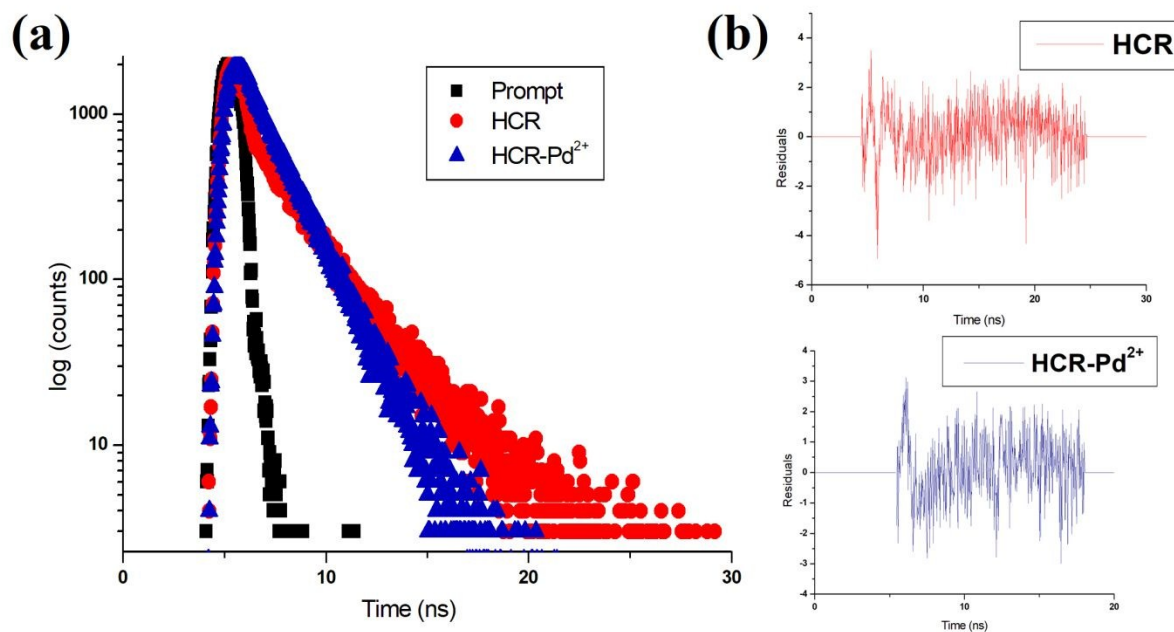


Fig. 5 (a) Time resolved fluorescence decay of HCR in the absence and presence of Pd²⁺ in the medium already mentioned; **(b)** corresponding residual plot ($\lambda_{\text{ex}}=450$ nm).

To further explore the selectivity of **HCR** for Pd²⁺, competition experiments are performed in the presence of Pd²⁺ mixed with 2.0 equiv. of each of the guest cations. **Fig. 7** shows that these free cations would have no such influence towards **HCR** and do not hamper the fluorogenic detection of Pd²⁺. Thus, coexisting metal ions do not significantly influence the recognition of Pd²⁺ by **HCR**.

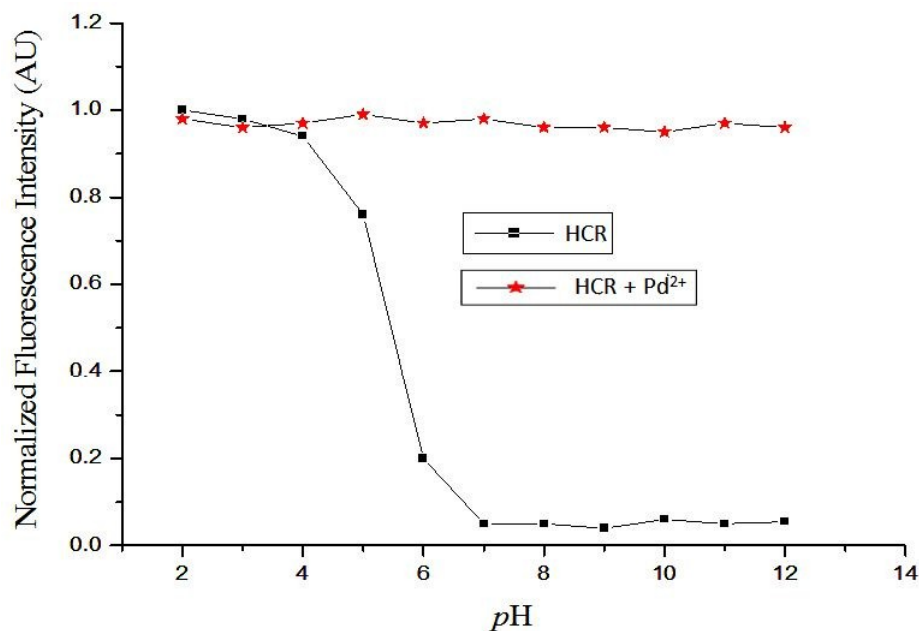


Fig.6 Variation of normalized fluorescence intensity of (HCR) and [CR-Pd²⁺]⁺ in EtOH/ H₂O (8:2, v/v) ($\lambda_{ex} = 545 \text{ nm}$, $\lambda_{em} = 598 \text{ nm}$) with change in pH.

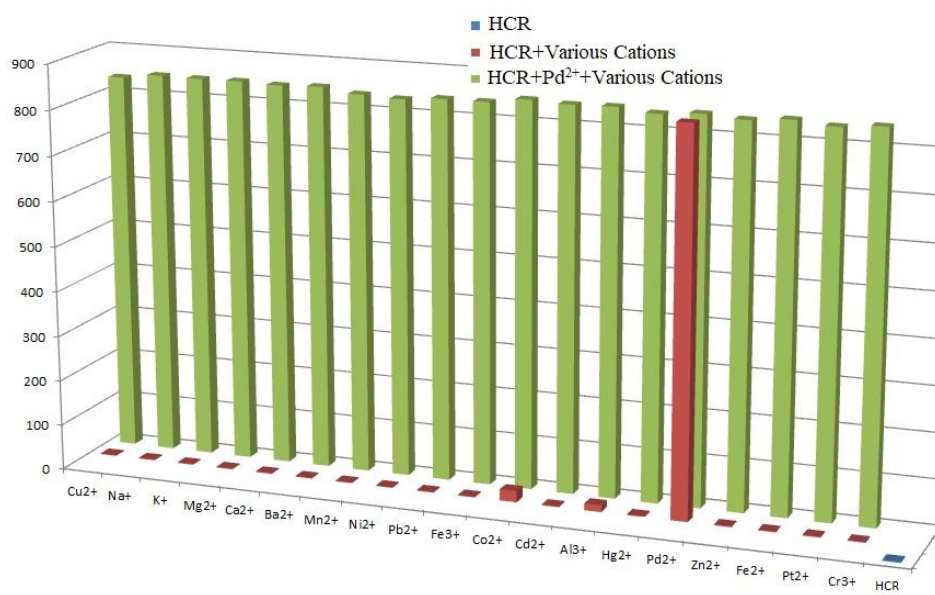


Fig. 7 Fluorescence intensity change of 20 μM HCR in EtOH/ H₂O (8:2, v/v) by Pd²⁺ ion at pH 7.2 in presence of competing metal ions.

3.4 Proposed binding mode

Job's method of continuous variation has yielded, from the absorption spectral data, a 1:1 (**HCR**: Pd²⁺) stoichiometry for the complex (**ESI**†, **Fig. S6**). The association constant (K_a) of the sensor with Pd²⁺ ion has been found to be $9.1 \times 10^4 \text{ M}^{-1}$ from Benesi–Hildebrand equation, using emission titration data (**ESI**†, **Fig. S7**). In FTIR spectrum of the sensor a broad peak at 3444 cm^{-1} for –OH (**HCR**) disappears in the complex [**CR**-Pd²⁺]⁺ (**ESI**†, **Fig. S8**) which refers to the binding of ligand to Pd(II) through oxygen of –OH *via* deprotonation. In the ESI-MS experiment, free **HCR** shows a signal at $m/z = 671.16 \text{ [M+H]}^+$; after completion of the reaction of Pd²⁺ with **HCR**, ESI-MS spectrum showed a clear base peak at 775.1075 [M]^+ (**ESI**†, **Fig. S9**); and which certainly corresponds to the formation of the complex, [**CR**-Pd²⁺]⁺. All these results suggest that the coordination cavity generated by coumarin-rhodamine dyad with hydroxy-O and imine-N chelator causes the binding of Pd²⁺ resulting in the four-coordinated [**CR**-Pd²⁺]⁺ complex by inducing opening of the spirolactam ring (**Scheme 1**). It is reported⁴⁵⁻⁴⁸ that the opening of spirolactam ring of rhodamine moiety enhances the emission intensity. This is happened due to the increase in conjugation in the ring-open form than in the ring-closed form which decreases the HOMO-LUMO energy gap from the free sensor to its Pd(II) complex and thereby the proposed mechanism will be as shown in **Scheme 1**.

3.5 Theoretical studies

The geometry generated by DFT for [**CR**-Pd²⁺]⁺ shows distorted square planar about Pd²⁺ ion where **HCR** acts as O,N,N,O chelator. The calculated Pd–O (rhodamine), Pd–N (imine), Pd–O (Coumarinyl) and Pd–N (rhodamine) distances are 2.48, 1.97, 2.20 and 2.48 Å respectively and are comparable with similar reported structure.^{49,50} Upon coordination the shortening of C–O (coumarinyl) distance, 1.38 to 1.32 Å, and elongation of the distances C–O

(spiro lactam) 1.25 to 1.30 Å and imine C=N, 1.27 to 1.30 Å have been calculated. Upon chelation of Pd²⁺ ion with the **HCR**, the energy of HOMO and LUMO are decreased relative to those of free **HCR**. (ESI[†], Fig. S1, S2). The HOMO–LUMO energy gap in **HCR** is 2.91 eV (≡ 426 nm) while that in the complex [CR–Pd²⁺]⁺ is 2.32 eV (≡ 535 nm). These are well in agreement with the experimentally observed longest wavelength absorption bands of **HCR** and [CR–Pd²⁺]⁺ respectively (Fig. 2). This supports the fact that the appearance of the intense 565 nm absorption band upon addition of Pd²⁺ is due to the formation of an entirely new species, the [CR–Pd²⁺]⁺ complex.

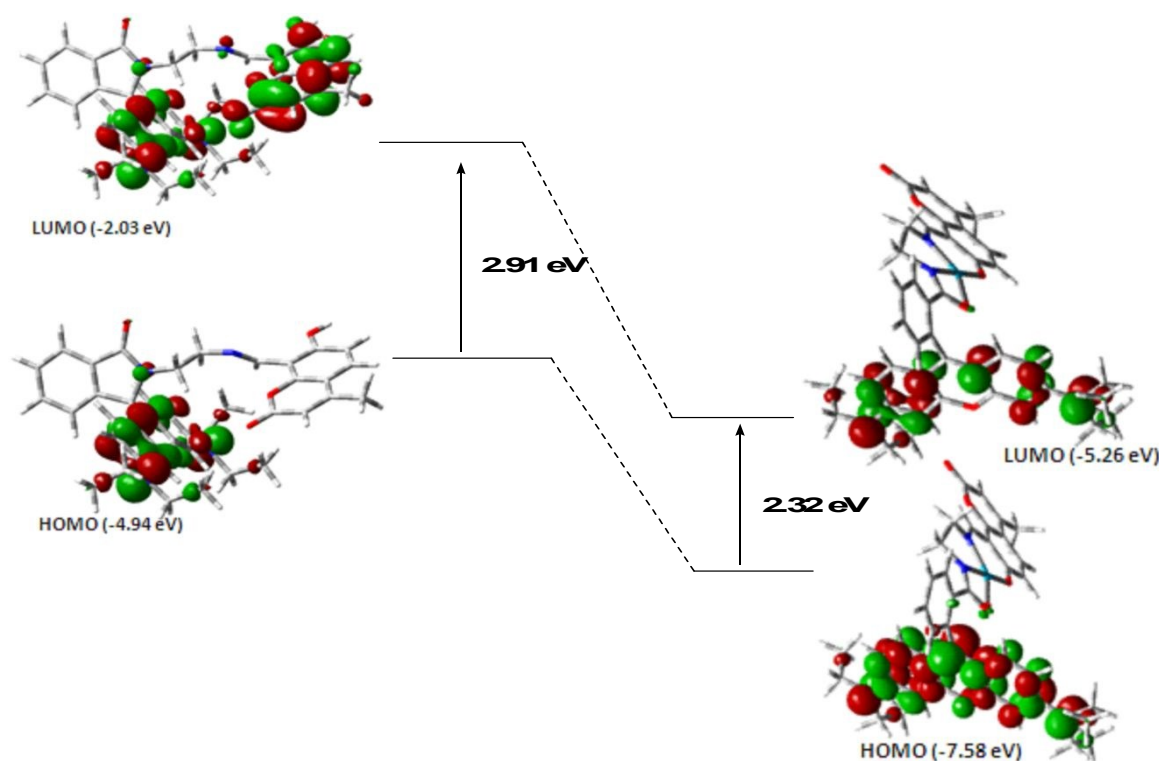


Fig. 8: HOMO–LUMO transitions of **HCR** and [CR–Pd²⁺]⁺ complex.

3.6 Intracellular imaging of Pd²⁺

1
2
3 Above experiments establish the unique selectivity and extreme sensitivity of **HCR** to Pd²⁺ with
4 very low detection limit (18.8 nM), we were interested to check the potential utility of the sensor
5 in living cells. Therefore, we have first checked the toxicity of the ligand in MCF-7 (breast
6 cancer cell line) upto 200 μM. Sensor shows toxicity after 25 μM (**Fig. 9**) and can be used as an
7 anti-cancer agent. Following fluorescence microscopic technique the detection of Pd²⁺ at very
8 low concentration has been examined in living cells. Palladium (0, II, IV) is a useful catalyst in
9 organic synthesis and the final product may contain traces of Pd(II) even after thorough repeated
10 purification. Such contamination of Pd is known to cause irritation of skin, eye, respiratory tract;
11 Pd(II) complexes are reportedly toxic and carcinogenic.⁵¹ For Pd, with a lethal dose of 5 – 10
12 ppm⁵¹⁻⁵³, the WHO recommendation for maximum uptake is restricted to ~1.5 – 15 μg/day.
13 Thus development of highly specific Pd²⁺ detection technique in live cells is an important
14 requirement of current research. In the present work, the cells were incubated with 5.0 μM of
15 **HCR** for 3h at 37°C and then treated with PdCl₂ (5 μM) for 30 min at the same temperature,
16 which resulted in red fluorescence (**Fig 10**). The red emission indicates that **HCR** is easily
17 entered into cell membrane and capable to image Pd²⁺ in living cells. It may, therefore, be
18 concluded that in both *in vitro* and *in vivo* sensing and in whole cell imaging of Pd²⁺, the **HCR** is
19 a potential analytical reagent. Moreover, a control experiment has also been performed to check
20 whether the spiro ring remains intact in the cell culture medium or not. The cells were treated
21 with **HCR** (5μM) for 24 h but did not get any sign of red coloration from the cells. This result
22 suggests that even in the complicated biological medium, the spiro ring of **HCR** does not open
23 (**ESI†, Fig. S10**).

24
25
26
27
28
29
30
31
32
33
34
35
36
37
38
39
40
41
42
43
44
45
46
47
48
49
50
51
52
53
54
55
56
57
58
59
60

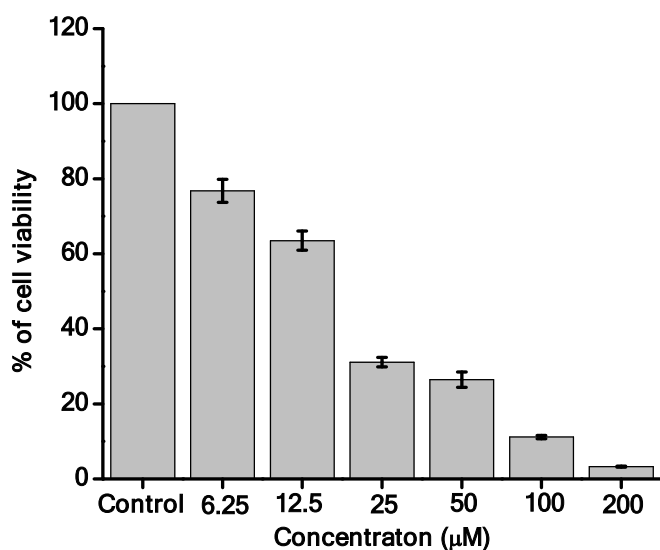


Fig. 9: Cell viability test by MTT assay by adding **HCR** to the media.

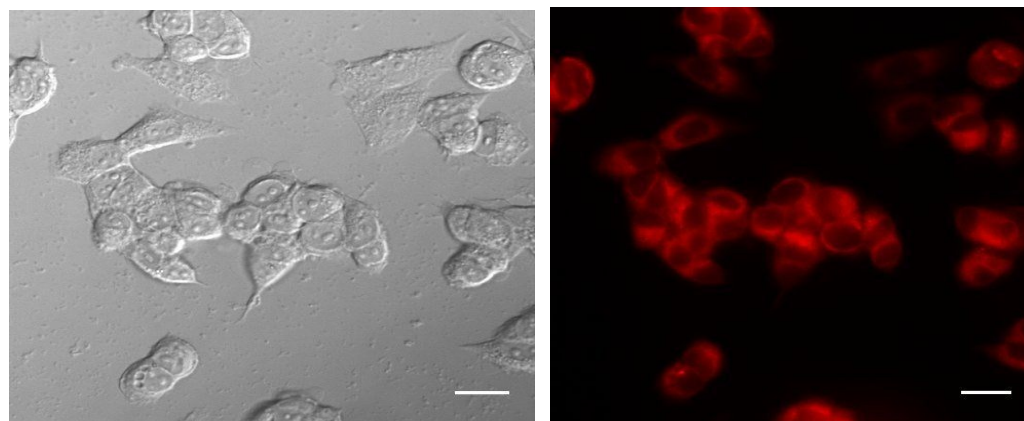


Fig. 10: Image of MCF7 Cells after the treatment with compound with Pd^{2+} .

4. Conclusion

The synthesized coumarinyl-rhodamine dyad (**HCR**) has served as highly efficient fluorescent sensor (λ_{em} , 598 nm) for quantitative detection of Pd^{2+} in semi-aqueous solution in presence of many other metal ions with a very low detection limit of 18.8 nM. The selectivity has been demonstrated by fluorescence, absorption and mass spectroscopy. The fluorescence intensity of

the sensor has been enhanced 270 times by adding Pd²⁺ to it *via* opening of ring of the spiro lactam form of rhodamine moiety. This sensor acts as a dual probe for detecting visually Pd²⁺ ions *via* the change in fluorescence and color. Due to high selectivity of HCR to Pd²⁺ in physiological medium at intracellular level, it can be used for identification of breast cancer cell.

Acknowledgements

Financial support from the Council of Scientific and Industrial Research (CSIR, Sanction no. 01(2814)/17/EMR-II.), New Delhi, India is gratefully acknowledged. Dr. Madhumita Manna, Principle, Bidhannagar College has acknowledged for her enormous moral support and encouragement. One of the authors (R.P.) is thankful to Department of Science and Technology (DST), Govt. of India for providing DST-INSPIRE research fellowship.

References:

- (a) L. Pu, Chem. Rev., 2004, **104**, 1687-1716. (b) V. Amendola, L. Fabbrizzi, F. Forti, M. Licchelli, C. Mangano, P. Pallavicini, A. Poggi, D. Sacchi and A. Taglietti, Coord. Chem. Rev., 2006, **205**, 273-299. (c) E. M. Nolan and S. J. Lippard, Chem. Rev., 2008, **108**, 3443-3480.
- (a) J. F. Zhang, Y. Zhou, J. Yoon and J. S. Kim, Chem. Soc. Rev., 2011, **40**, 3416-3429.
(b) Z. Xu, X. Chen, H. N. Kim and J. Yoon, Chem. Soc. Rev., 2010, **39**, 127-137
(c) R. Balamurugan, C.C. Chien, K.M. Wu, Y.-H. Chiu and Jui-Hsiang Liu, Analyst, 2013, **138** 1564-1569.
- (a) H. Kim, K. S. Moon, S. Shim and J. Tae, Chem. Asian J. 2011, **6**, 1987-1991. (b) H. Li, J. Fan, J. Du, K. Guo, S. Sun, S. Liu and X. Peng, Chem. Commun., 2010, **46**, 1079-1081.
- (a) H. Li, J. Fan, F. Song, H. Zhu, J. Du, S. Sun and X. Peng, Chem.–Eur. J., 2010, **16**, 12349-12356. (b) D. Keum, S. Kim and Y. Kim, Chem. Commun., 2014, **50**, 1268-1270.

- 1
2
3 5 (a) M. Ware, *Platinum Metals Review*, 2005, **49**, 190-195. (b) T. Iwasawa, M. Tokunaga, Y.
4 Obora and Y. Tsuji, *J. Am. Chem. Soc.*, 2004, **126**, 6554-6555. (c) K. Köhler, W. Kleist and S.
5
6 S. Proćki, *Inorg. Chem.*, 2007, **46**, 1876-1879. (d) C.M. Crudden, M. Sateesh and R. Lewis, *J.*
7
8
9
10
11
12
13 6 (a) S. L. Buchwald, C. Mauger, G. Mignani and U. Scholze, *Adv. Synth. Catal.*, 2006, **348**,
14 23-29. (b) X. Chen, K. M. Engle, D. H. Wang and J. Q. Yu, *Angew. Chem.*, 2009, **121**, 5196-
15 5217.
16
17
18
19
20
21
22 7 (a) J. Kielhorn, C. Melber, D. Keller and I. Mangelsdorf, *Int. J. Hyg. Environ. Health*, 2002,
23 **205**, 417-432. (b) C. D Spicer, T. Triemer and B. G. Davis, *J. Am. Chem. Soc.*, 2012, **134**, 800-
24 803.
25
26
27
28
29
30
31
32
33 8 T. Gebel, H. Lantsch, K. Plebow and H. Dunkelberg, *Mutat. Res. Genet. Toxicol. Environ.*
34
35
36
37
38
39
40
41
42 9 T. Z. Liu, S. D. Lee and R. S. Bhatnagar, *Toxicol. Lett.*, 1979, **4**, 469-473.
43
44
45
46
47
48
49
50
51
52 10 J. Kielhorn, C. Melber, D. Keller and I. Mangelsdorf, *Int. J. Hyg. Environ. Health*, 2002, **205**,
53 417-432.
54
55
56
57
58
59
60 11 B. Dimitrova, K. Benkhedda, E. Ivanova and F. Adams, *J. Anal. At. Spectrom.*, 2004, **19**,
1394-1396.
12 C. Locatelli, D. Melucci and G. Torsi, *Anal. Bioanal. Chem.*, 2005, **382**, 1567-1573..
13 K. Van Meel, A. Smekens, M. Behets, P. Kazandjian and R. Van Grieken, *Anal. Chem.*,
2007, **79**, 6383-6389.
14 (a) H. Li, J. Fan and X. Peng, *Chem. Soc. Rev.*, 2013, **42**, 7943-7962. (b) J. Du, M. Hu, J.
Fan and X. Peng, *Chem. Soc. Rev.*, 2012, **41**, 4511-4535.

- 1
2
3 15 (a) L. Duan, Y. Xu and X. Qian, *Chem. Commun.*, 2008, **0**, 6339-6341. (b) J. R. Matthews,
4 F. Goldoni, H. Kooijman, A. L. Spek, A. P. H. J. Schenning and E. W. Meijer, *Macromol Rapid*
5 *Commun.*, 2007, **28**, 1809-1815.
6
7
8
9
10 16 (a) A. K. Mahapatra, S. K. Manna, K. Maiti, S. Mondal, R. Maji, D. Mandal, S. Mandal, M. R.
11 Uddin, S. Goswami, C.K. Quah and H. Fun, *Analyst*, 2015, **140**, 1229-1236. (b) S. Goswami, D.
12 Sen, N.K. Das, H. Fun and C. K. Quah, *Chem. Commun.*, 2011, **47**, 9101–9103.
13
14
15
16
17 17 G. Wei, L. Wang, J. Jiao, J. Hou, Y. Cheng and C. Zhu, *Tetrahedron Lett.*, 2012, **53**, 3459–
18 3462.
19
20
21 18. (a) Y. K. Yang, Yook, K. J.; Tae, J. J. *Am. Chem. Soc.*, 2005, **127**, 16760-16761. (b) J. Y.
22 Kwon, Y. J. Jang, Y. J. Lee, K. M. Kim, M. S. Seo, W. Nam, J. Yoon, *J. Am. Chem.*
23 *Soc.*, 2005, **127**, 10107-10111. (c) V. Dujols, F. Ford, A. W. Czarnik, *J. Am. Chem.*
24 *Soc.*, 1997, **119**, 7386-7387. (d) M. Wang, X. Liu, H. Lu, H. Wang, and Z. Qin, *ACS Appl.*
25 *Mater. Interfaces* 2015, **7**, 1284–1289. (e) R. Balamurugan, J. –H. Liu, B. –T. Liu, *Coord. Chem.*
26 *Rev.*, 2018, **376**, 196-224. (f) N. Kumari, N. Dey, K. Kumar and S. Bhattacharya, *Chem. Asian J.*
27 2014, **9**, 3174 – 3181. (g) H. Li, J. Cao, H. Zhu, J. Fan, X. Peng, *Tet. Lett.*, 2013, **54**, 4357–4361
28
29
30
31
32
33
34
35
36
37
38 19 A. K. Bhanja, S. Mishra, K. Das Saha and C. Sinha, *Dalton Trans.*, 2017, **46**, 9245–9252.
39
40
41 20. A. K. Bhanja, S. Mishra, K. Kar, K. Naskar, S. Maity, K. Das Saha and C. Sinha, *New J.*
42 *Chem.*, 2018, **42**, 17351-17358.
43
44
45 21 Jacob Q. Umberger and Victor K. LaMer, *J. Am. Chem. Soc.*, 1945, **67**, 1099–1109.
46
47
48 22 K. Das, U. Panda, A. Datta, S. Roy, S. Mondal, C. Massera, T. Askun, P. Celikboyun, E.
49 Garribba, C. Sinha, K. Anand, T. Akitsu and K. Kobayashi, *New J. Chem.*, 2015, **39**, 7309-7321.
50
51
52 23 J.-S. Wu, I.-C. Hwang, K. S. Kim and J. S. Kim, *Org. Lett.*, 2007, **9**, 907–910.
53
54
55
56
57
58
59
60

- 1
2
3 24 M. J. Frisch, G. W. Trucks, H. B. Schlegel, G. E. Scuseria, M. A. Robb, J. R. Cheeseman, G.
4 Scalmani, V. Barone, B. Mennucci, G. A. Petersson, H. Nakatsuji, M. Caricato, X. Li, H. P.
5 Hratchian, A. F. Izmaylov, J. Bloino, G. Zheng, J. L. Sonnenberg, M. Hada, M. Ehara, K.
6 Toyota, R. Fukuda, J. Hasegawa, M. Ishida, T. Nakajima, Y. Honda, O. Kitao, H. Nakai, T.
7 Vreven, J. A. Montgomery Jr., J. E. Peralta, F. Ogliaro, M. Bearpark, J. J. Heyd, E. Brothers, K.
8 N. Kudin, V. N. Staroverov, R. Kobayashi, J. Normand, K. Raghavachari, A. Rendell, J. C.
9 Burant, S. S. Iyengar, J. Tomasi, M. Cossi, N. Rega, J. M. Millam, M. Klene, J. E. Knox, J.
10 B. Coss, V. Bakken, C. Adamo, J. Jaramillo, R. Gomperts, R. E. Stratmann, O. Yazyev, A. J.
11 Austin, R. Cammi, C. Pomelli, J. W. Ochterski, R. L. Martin, K. Morokuma, V. G. Zakrzewski,
12 G. A. Voth, P. Salvador, J. J. Dannenberg, S. Dapprich, A. D. Daniels, Ö. Farkas, J. B. Foresman,
13 J. V. Ortiz, J. Cioslowski and D. J. Fox, Gaussian 09, Revision D.01, Gaussian Inc., Wallingford,
14 CT, 2009.
15
16 25 A. D. Becke, *J. Chem. Phys.*, 1993, **98**, 5648-5652.
17
18 26 C. Lee, W. Yang and R. G. Parr, *Phys. Rev. B: Condens. Matter*, 1988, **37**, 785–789.
19
20 27 P. J. Hay and W. R. Wadt, *J. Chem. Phys.*, 1985, **82**, 270–283.
21
22 28 W. R. Wadt and P. J. Hay, *J. Chem. Phys.*, 1985, **82**, 284–298.
23
24 29 P. J. Hay and W. R. Wadt, *J. Chem. Phys.*, 1985, **82**, 299–305.
25
26 30 V. Barone and M. Cossi, *J. Phys. Chem. A*, 1998, **202**, 1995–2001.
27
28 31 M. Cossi and V. Barone, *J. Chem. Phys.*, 2001, **115**, 4708–4717.
29
30 32 M. Cossi, N. Rega, G. Scalmani and V. Barone, *J. Comput. Chem.*, 2003, **24**, 669-681.
31
32 33 N. M. O’Boyle, A. L. Tenderholt and K. M. Langner, *J. Comput. Chem.*, 2008, **29**, 839–845.
33
34 34 A. K. Mahapatra, S. K. Manna, K. Maiti, S. Mondal, R. Maji, D. Mandal, S. Mandal, Md. R.
35 Uddin, S. Goswami, C. K. Quah and H. K. Fun, *Analyst*, 2015, **140**, 1229–1236.
36
37
38
39
40
41
42
43
44
45
46
47
48
49
50
51
52
53
54
55
56
57
58
59
60

- 1
2
3 35 F. Liu, J. Du, M. Xu and G. Sun, Chem. Asian J., 2016, **11**, 43-48.
4
5 36 Q. Huang, Y. Zhou, Q. Zhang, E. Wang, Y. Min, H. Qiao, J. Zhang and T. Ma, Sens.
6 Actuators B:, 2015, **208**, 22–29.
7
8 37 Y. Chen, B. Chen and Y. Han, Sens. Actuators B:, 2016, **237**, 1–7.
9
10 38 V. Sharma, A. K. Sainib and S. M. Mobin, J. Mater. Chem. B, 2016, **4**, 2466–2476.
11
12 39 J. Panchompoo, L. Aldous, M. Baker, M. I. Wallace and R. G. Compton, Analyst, 137 (2012,
13 **137**, 2054–2062.
14
15 40 W. Liu, J. Jiang, C. Chen, X. Tang, J. Shi, P. Zhang, K. Zhang, Z. Li, W. Dou, L. Yang and
16 W. Liu, Inorg. Chem., 2014, **53**, 12590–12594.
17
18 41 F. Song, A. L. Garner and K. Koide, J. Am. Chem. Soc., 2007, **129**, 12354–12355.
19
20 42 D. Keum, S. Kim and Y. Kim, Chem. Commun., 2014, **50**, 1268–1270.
21
22 43 P. Kumar, V. Kumar and R. Gupta, RSC Adv., 2017, **7**, 7734–7741.
23
24 44 W. X. Ren, T. Pradhan, Z. Yang, Q. Y. Cao and J. S. Kim, Sens. Actuators B:, 2012, **171**,
25 1277–1282.
26
27 45 S. Sun, B. Qiao, N. Jiang, J. Wang, S. Zhang and X. Peng, Org. Lett., 2014, **16**, 1132–1135.
28
29 46 S. Goswami, D. Sen, N. Kumar Das, H. K. Fun and C. K. Quahb, Chem. Commun., 2011,**47**,
30 9101-9103.
31
32 47 M. A. Bennett, S. K. Bhargava, M. A. Keniry, S. H. Prive'r, P. M. Simmonds, J. Wagler and
33 A. C. Willis, Organometallics, 2008, **27**, 5361-5370.
34
35 48 U. Reddy G., F. Ali, N. Taye, S. Chattopadhyay and A. Das, Chem. Commun., 2015, **51**,
36 3649-3652.
37
38
39
40
41
42
43
44
45
46
47
48
49
50
51
52
53
54
55
56
57
58
59
60

1
2
3 49 B. Liu, H. Wang, T. Wang, Y. Bao, F. Du, J. Tian, Q. Li and R. Bai, Chem. Commun., 2012,
4
5 **48**, 2867–2869.

6
7
8 50 X. Wang, Z. Guo, S. Zhu, H. Tian and W. Zhu, Chem. Commun., 2014, **50**, 13525–13528.

9
10 51 C. E. Garrett, K. Prasad, Adv. Synth. Catal., 2004, **346**, 889–900.

11
12
13 52 D. G. Cho and J. L. Sessler, Chem. Soc. Rev., 2009, **38**, 1647–1662.

14
15
16 53 F. Song, A.L. Garner and K. Koide, J. Am. Chem. Soc., 2007, **129**, 12354–12355.
17
18
19
20
21
22
23
24
25
26
27
28
29
30
31
32
33
34
35
36
37
38
39
40
41
42
43
44
45
46
47
48
49
50
51
52
53
54
55
56
57
58
59
60

Pictorial abstract

Fluorescence sensing and intracellular imaging of Pd²⁺ ion by a novel coumarinyl-rhodamine Schiff base†

Arup Kumar Adak,^a Rakesh Purkait^b, Saikat Manna,^c Bankim Chandra Ghosh,^d Sudipta Pathak^c
and Chittaranjan Sinha^b

